2005 American Control Conference
June 8-10, 2005. Portland, OR, USA

Population Modeling for Ethanol Productivity Optimization in Fed-Batch Yeast Fermenters

Jared Hjersted and Michael A. Henson
Department of Chemical Engineering
University of Massachusetts
Amherst, MA 01003-3110

Abstract— **We develop a population model that captures the cell cycle dependent production of ethanol in fed-batch yeast cultures. The dynamic model is used to compute fed-batch operating policies that maximize total ethanol production. The initial volume and glucose concentration, the feed flow rate and glucose feed concentration profiles, and the final batch time are treated as decision variables in the dynamic optimization problem. Optimal solutions computed with different ethanol production rates in the G1, S and G2/M cell cycle phases are compared. We find that the optimal solutions are insensitive to the production rate values unless ethanol is assumed to be produced only in the G1 phase. The implications of the observed cell cycle production dependencies on metabolite productivity optimization are discussed.**

I. INTRODUCTION

The yeast *Saccharomyces cerevisiae* is commonly used as a host organism for the production of recombinant proteins because it has transcription, translation and secretion systems similar to those in higher eukaryotes [1]. Notable examples of heterologous proteins industrially produced with *S. cerevisiae* include human interferon, hepatitis B surface antigen and insulin [2]. While most native yeast proteins are synthesized at a constant rate throughout the cell cycle, several recombinant proteins have been shown to be preferentially synthesized and/or secreted during a specific cell cycle phase [3], [4]. Cell cycle dependent protein production appears to be even more common in mammalian cells such as hydridomas [5] and Chinese hamster ovary (CHO) cells [6]. While several investigators have proposed that the tendency of some proteins to be differentially produced during the cell cycle could be exploited to enhance protein production [3], [7], this concept has not been systematically investigated. We have initiated a research project which aims to combine population balance equation (PBE) models and dynamic optimization to enhance the production of cell cycle dependent proteins in fed-batch cultures. As a preliminary step towards this goal, in this paper we consider the problem of ethanol optimization in fed-batch yeast fermenters. Ethanol is known to be secreted primarily by large budded cells [8], [9]. Therefore ethanol synthesis serves as a convenient model system to study proteins that are preferentially produced during the late S, G2 and M phases of the cell cycle.

To who correspondence should be addressed: E-mail: henson@ecs.umass.edu

We previously developed a mass structured PBE model that captures the cell cycle dependency of ethanol production [10]. The PBE model was formulated by assuming that single cells metabolize nutrients via three metabolic pathways: glucose fermentation, glucose oxidation and ethanol oxidation. Ethanol produced by the fermentative pathway was assumed to be utilized as a carbon source only at sufficiently low glucose concentrations [11]. The single cell growth rate for each metabolic pathway was assumed to follow Monod kinetics with respect to the nutrients involved. The cell cycle dependency of ethanol production was included in the ethanol formation rate associated with glucose fermentation. Discretization of the PBE model in the mass domain using orthogonal collocation on finite elements produced a set of ordinary differential equations (ODEs) suitable for numerical integration. A converged solution was obtained with 109 collocation points, yielding a discretized model comprised of 117 ODEs.

The transient nature of fed-batch operation requires that the optimal nutrient feeding policy be determined by solving a dynamic optimization problem [12]. The prototypical problem involves the use of a dynamic model to compute the optimal policy followed by the design of a feedback controller that provides tracking of the optimal trajectory [13]. The formulation and solution of dynamic optimization problems for maximizing productivity in fed-batch bioreactors has been extensively studied for several decades [14], [15]. While optimal control strategies for maximizing protein production have been presented, most methods are based on simple unsegregated models that are incapable of describing cell cycle dependent production. One notable exception is a study in which a simple cell cycle model was used to determine optimal fed-batch operating policies for rice α-amylase production by a recombinant yeast [7].

The development of fed-batch optimization strategies based on PBE models is considerably more challenging. Dynamic optimization codes usually require that the process model be posed as a set of nonlinear algebraic constraints [16], thereby necessitating both spatial and temporal discretization of the PBE model. The size of the resulting optimization problem will be several orders of magnitude larger than that encountered with a simple unsegregated model. To our knowledge the use of PBE models to compute optimal fed-batch operating policies has not been explored. In this paper we take a preliminary step towards

0-7803-9098-9/05/$25.00 ©2005 AACC

this goal by computing optimal open-loop feeding policies using a simple population model that captures cell cycle dependent ethanol production. The model accounts for cell growth and ethanol production/consumption via the glucose fermentative, glucose oxidative and ethanol oxidative pathways. The dynamic optimization problem is formulated as maximization of ethanol production subject to constraints imposed by the temporally discretized model equations. In addition to the feed flow rate and glucose feed concentration profiles, the initial volume, initial glucose concentration and final batch time are treated as decision variables.

II. POPULATION MODEL FOR CELL CYCLE DEPENDENT ETHANOL PRODUCTION

The population model is based on a very simple description of the eukaryotic cell cycle in which cells are distributed in the G1, S and G2/M phases [7]. Transitions between cell cycle phases are described by the following equations:

$$\frac{dX_{G1}}{dt} = -P_{G1}X_{G1} + 2P_M X_M \quad (1)$$

$$\frac{dX_S}{dt} = -P_S X_S + P_{G1}X_{G1} \quad (2)$$

$$\frac{dX_M}{dt} = -P_M X_M + P_S X_S \quad (3)$$

where the subscripts $G1$, S and M are used to denote the cell cycle phase, X is the number of cells in a particular phase and P is the transition rate between two phases. The cell fraction ϕ in each phase is defined as:

$$\phi_{G1} = \frac{X_{G1}}{Z}, \qquad \phi_S = \frac{X_S}{Z}, \qquad \phi_M = \frac{X_M}{Z} \quad (4)$$

The total cell number $Z = X_{G1} + X_S + X_M$ is assumed to increase exponentially:

$$\frac{dZ}{dt} = \mu Z \quad (5)$$

where the overall growth rate μ depends on carbon source availability. We utilize the following expressions that relate the cell fractions in the three cell cycle phases to the growth rate:

$$\phi_{G1} = \exp(\beta\mu) \quad (6)$$

$$\phi_S = \frac{0.33\mu}{\ln 2} \quad (7)$$

$$\phi_M = 1 - \phi_{G1} - \phi_S \quad (8)$$

where β is an adjustable parameter. Although derived under the assumption of balanced growth, the following relations relating the cell fractions ϕ and the transition rates P have been shown to hold for unbalanced growth conditions [7]:

$$P_{G1} = (2/\phi_{G1} - 1)\mu \quad (9)$$

$$P_S = (1/\phi_S + \phi_M/\phi_S)\mu \quad (10)$$

$$P_M = \mu/\phi_M \quad (11)$$

The overall growth rate μ is determined by the contributions of the glucose fermentative (gf), glucose oxidative (go) and ethanol oxidative (eo) pathways [10]:

$$\mu(G,E) = \mu_{gf}(G) + \mu_{go}(G) + \mu_{eo}(G,E) \quad (12)$$

where G and E denote the extracellular concentrations of glucose and ethanol, respectively. Fermentation is assumed to be inhibited by high glucose concentrations according to the Crabtree effect [17]. The dissolved oxygen concentration is assumed to be regulated as a constant value such that the growth rate expressions for the two oxidative pathways depend only on the carbon sources. Because glucose is the preferred carbon source, ethanol oxidation is assumed to inhibited by high glucose concentrations. The resulting growth rate expressions are:

$$\mu_{gf}(G) = \frac{\mu_{mgf}G}{K_{gf} + G + \frac{G^2}{K_{igf}}} \quad (13)$$

$$\mu_{go}(G) = \frac{\mu_{mgo}G}{K_{go} + G} \quad (14)$$

$$\mu_{eo}(G,E) = \frac{\mu_{meo}E}{K_{eo} + E}\frac{K_{ieo}}{K_{ieo} + G} \quad (15)$$

Extracellular balances yield the following equations:

$$\frac{dV}{dt} = F \quad (16)$$

$$\frac{d(VG)}{dt} = FG_f - \left(\frac{\mu_{gf}}{Y_{gf}} + \frac{\mu_{go}}{Y_{go}}\right)Z \quad (17)$$

$$\frac{d(VE)}{dt} = \left[\psi(X_{G1}, X_S, X_M, Z)\frac{\mu_{gf}}{Y_{gf}} - \frac{\mu_{eo}}{Y_{eo}}\right]Z \quad (18)$$

where V is the reactor volume, F is the feed flow rate and Y are yield coefficients for the three pathways. The function ψ accounts for cell cycle dependent ethanol production via the fermentation pathway:

$$\psi(X_{G1}, X_S X_M, Z) = \frac{\rho_{G1}X_{g1} + \rho_S X_S + \rho_M X_M}{Z} \quad (19)$$

where ρ represents is the specific ethanol production rate in a particular cell cycle phase. While specific production rate values have been estimated for α-amylase production [7], we simply adjusted the ρ parameters to evaluate the effect of different cell cycle production dependencies on the computed nutrient feeding policies.

The nominal model parameter values listed in Table I were generated from several sources. The maximum growth rate (μ_{mgf}) and glucose inhibition constant (K_{igf}) for glucose fermentation were obtained from Henson and Seborg [18]. Maximum growth rates for the other two pathways (μ_{meo}, μ_{mgo}) were calculated by scaling the values given in Mhaskar *et al.* [10] to be consistent with the μ_{mgf} value. The saturation constants (K_{gf}, K_{eo}, K_{go}) and the glucose inhibition constant for ethanol oxidation (K_{ieo})

TABLE I

NOMINAL MODEL PARAMETER VALUES.

Variable	Value	Variable	Value
μ_{mgf}	0.48 h^{-1}	K_{gf}	40 g/l
K_{igf}	20 g/l	Y_{gf}	1.04×10^{11} g^{-1}
μ_{meo}	0.112 h^{-1}	K_{eo}	1.3 g/l
K_{ieo}	0.4 g/l	Y_{eo}	3.47×10^{11} g^{-1}
μ_{mgo}	0.052 h^{-1}	K_{go}	2.0 g/l
Y_{go}	4.51×10^{11} g^{-1}	β	-3.9
ρ_{G1}	0	ρ_S	0.75
ρ_M	0.5	$V(0)$	1 l
$V(t_f)$	5 l		

were obtained from the same source. The yield coefficients (Y_{gf}, Y_{eo}, Y_{go}) were calculated by scaling the values given in Mhaskar *et al.* [10] with the same single cell mass (1.44×10^{-12} g) used to the scale the maximum growth parameters. Uchiyama and Shioya [7] fit the β parameter to growth rate data for cell populations in the G1, S and G2/M phases. We used the same parameter value under the assumption that their recombinant yeast strain exhibits similar growth rate characteristics as a wild type strain used for ethanol production. The specific ethanol production rate values (ρ_{G1}, ρ_S, ρ_M) were chosen somewhat arbitrarily to reflect experimental data showing that ethanol is produced primarily by large budded cells [8]. A larger value was chosen for ρ_S than for ρ_M due to the relatively short duration of the S phase. These values were modified to evaluate the effect of different cell cycle dependencies on the optimal feeding policy.

III. FED-BATCH OPTIMIZATION STRATEGY

The objective function to be maximized was the total mass of ethanol produced at the end of the batch. The initial volume $V(0)$ and glucose concentration $G(0)$, the feed flow rate $F(t)$ and glucose feed concentration $G_f(t)$, and the final batch time t_f were treated as decision variables. Therefore the dynamic optimization problem had the form:

$$\max_{V(0),G(0),F(t),G_f(t),t_f} VE(t_f) \tag{20}$$

The maximization was performed subject to constraints imposed by the dynamic model equations and various operational restrictions. We utilized a simultaneous solution method that explicitly accounts for state dependent constraints and is applicable to large optimal control problems [16], [19]. The dynamic model equations were temporally discretized and posed as equality constraints. Model discretization was performed using orthogonal collocation on finite elements with 96 elements and 8 internal collocation points to yield a total of 865 node points.

The dynamic optimization problem was solved using the code IPOPT [20] within the AMPL modeling language. The following bounds were imposed on the problem variables:

$$0 \le F(t) \le 5 \text{ l/h}, \quad \left|\frac{df}{dt}\right| \le 1 \text{ l/h/h} \tag{21}$$

$$0 \le G_f(t) \le 100 \text{ g/l}, \quad \left|\frac{dG_f}{dt}\right| \le 50 \text{ g/l/h} \tag{22}$$

$$14.4 \text{ h} \le t_f \le 48 \text{ h}, \quad 0 \le G(0) \le 50 \text{ g/l} \tag{23}$$

$$V(0) \ge 1 \text{ l}, \quad V(t_f) \le 5 \text{ l} \tag{24}$$

$$X_{G1}, X_S, X_M, Z, V, G, E \ge 0 \tag{25}$$

Most bounds were specified to ensure that the optimal solution remained within a physically meaningful operating range. Derivative bounds were imposed on the feed variables to avoid undesirable solutions in which the feed flow rate rapidly cycled between its lower and upper bounds to achieve a minuscule improvement in the objective function. A lower bound on the batch time was implemented to avoid complications associated with using a variable number of finite elements. The optimization model consisted of 8647 decision variables and 6914 constraints.

IV. RESULTS AND DISCUSSION

To evaluate the impact of dynamic optimization the first set of results were generated by fixing the initial fermenter conditions, the feeding policy and the final batch time. The following operating conditions were simulated: $V(0)$ = 1 l, $G(0)$ = 50 g/l, $F(t)$ = 0.167 l/h, $G_f(t)$ = 100 g/l, and t_f = 24 h. Because the primary objective was to analyze the effect of a constant feed flow rate, the other variables were chosen to be close to their optimal values computed below. The nominal set of model parameter values listed in Table I were used. Figure 1 shows the glucose concentration and ethanol productivity over the fed-batch run. The constant feeding policy produced a highly variable glucose concentration and 70.6 g of ethanol at the end of the batch. Figure 2 shows the cell number in each cell cycle phase and the growth rate attributable to each metabolic pathway. Most cells were located in the G1 and M phases due to the relatively short duration of the S phase. For this feeding policy the fermentative pathway was dominant, the glucose oxidative pathway was significant and the ethanol oxidative pathway was negligible.

The next set of results were generated by solving the dynamic optimization problem under the assumption that ethanol is produced only in the S and M phases. As before the nominal parameter values listed in Table I were used. The optimal feeding policy is shown in Figure 3. The feed flow rate was maintained at zero for the first eight hours to achieve a glucose concentration that maximizes the fermentation rate. Then the feed rate was increased slowly to maintain the optimal glucose concentration before dropping abruptly near the end of the batch to ensure satisfaction of the terminal volume constraint. During the period of non-zero feed rate, the feed glucose concentration was placed at its upper bound to maximize the fermentation rate. When the derivative constraint on the feed flow rate was removed,

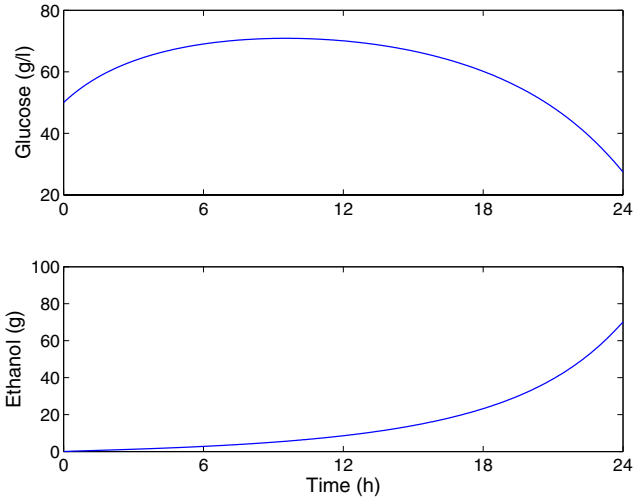

Fig. 1. Glucose concentration and ethanol productivity for a constant feed flow rate.

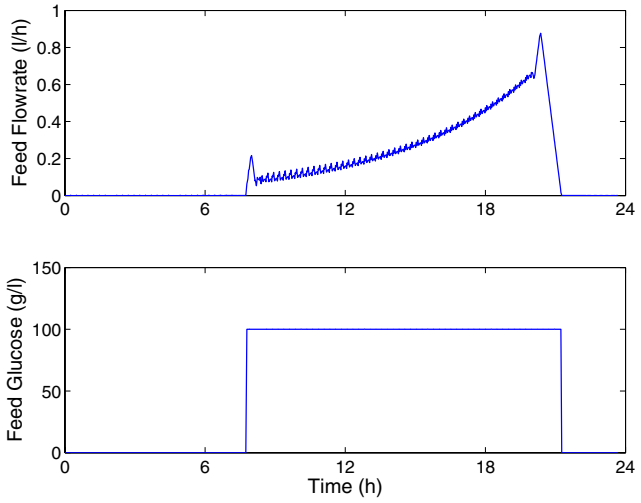

Fig. 3. Optimal feeding policy for ethanol production in the S and M cell cycle phases.

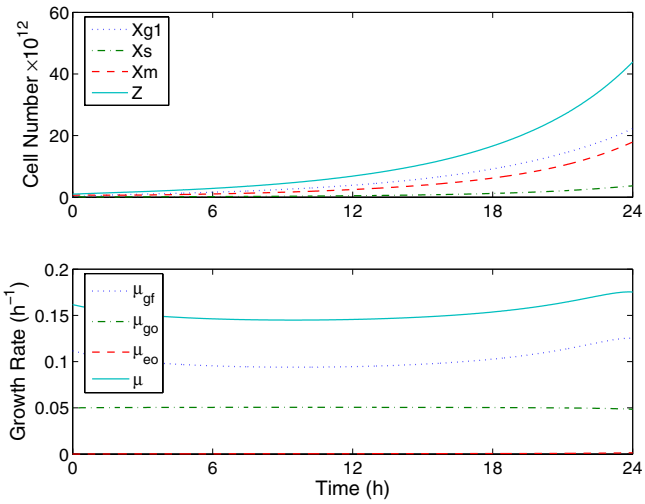

Fig. 2. Cell populations and growth rates for a constant feed flow rate.

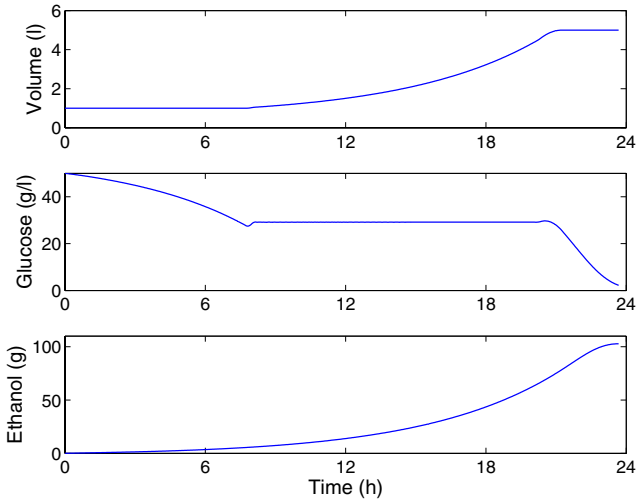

Fig. 4. Volume, glucose concentration and ethanol productivity obtained with the optimal feeding policy for ethanol production in the S and M cell cycle phases.

the small oscillations were replaced by violent oscillations in which the feed rate rapidly cycled between its lower and upper bounds to achieve a minuscule improvement in the objective function. This undesirable behavior was easily eliminated through the use of the feed rate derivative constraint.

Figure 4 shows the liquid volume, glucose concentration and ethanol productivity trajectories when ethanol production occurred in the S and M phases. The initial volume was set equal to the lower bound, while the upper bound was chosen for the initial glucose concentration. By driving the glucose concentration to the value that maximized the fermentation rate, the optimized solution produced 102.7 g of ethanol. This productivity represents a 45% improvement over that obtained with the constant feed flow rate.

Figure 5 shows the cell number in each cell cycle phase and the growth rate attributable to each metabolic pathway for this case. The fermentative and overall growth rates were larger than those achieved with the constant feed flow rate (see Figure 2). The higher growth rates were attributable to the optimized feeding policy that maintained the glucose concentration at a value that maximized fermentation relative to the other two metabolic pathways. The fermentative pathway was preferred for several reasons: (1) fermentation provided the largest growth rate of the three pathways; (2) higher growth rates shortened the G1 phase as per (6); and (3) ethanol was only produced via the fermentative pathway by cells in the S and M phases. Consequently the optimal operating policy for fermentation products such as ethanol that are synthesized in the later cell cycle phases is manipulation of the feeding rate to maximize

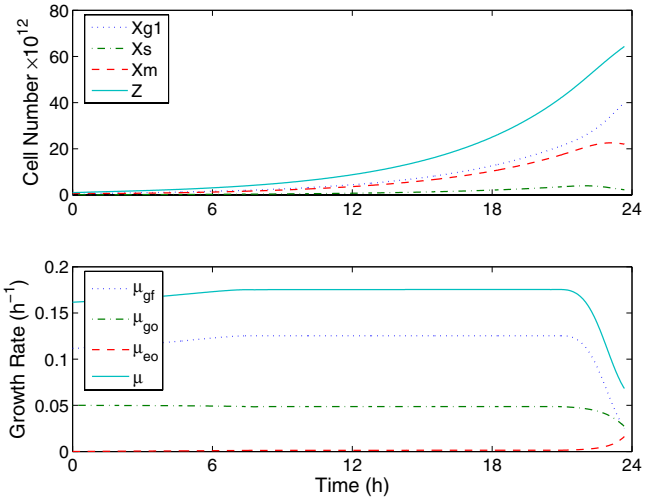

Fig. 5. Cell populations and growth rates obtained with the optimal feeding policy for ethanol production in the S and M cell cycle phases.

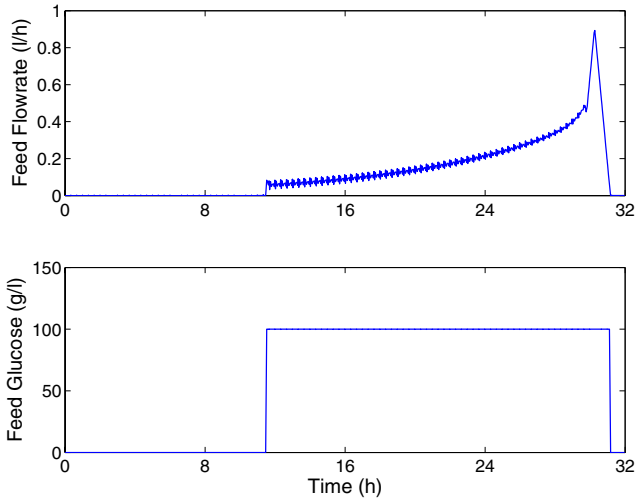

Fig. 6. Optimal feeding policy for metabolite production in the G1 cell cycle phase.

flux through the fermentative pathway while honoring the terminal volume constraint. We found that the optimal solution was not significantly affected by the values chosen for metabolite production rates unless ϕ_{G1} was much larger than both ϕ_S and ϕ_M. This result suggests that the proposed framework will be most beneficial for metabolites that are primarily produced in the G1 phase because only then will the optimal solution deviate substantially from that obtained with a standard model that neglects cell cycle production dependencies. This case is explored below.

The final set of results were generated with a different set of metabolite production rates ρ than those listed in Table I. Although not realistic for ethanol, the production rates were specified to represent a fermentation metabolite produced only during the G1 cell cycle phase: ϕ_{G1} = 0.462, ϕ_S = 0 and ϕ_M = 0. The ϕ_{G1} value was chosen such that the optimized solution produced the same amount of ethanol (102.7 g) as the previous case with ϕ_{G1} = 0. Otherwise the nominal parameter values listed in Table I were used. The optimal feeding policy is shown in Figure 6. The most significant differences with the optimal solution obtained for ϕ_{G1} = 0 were (see Figure 3): (1) the feed rate was initially maintained at zero for a longer period of time; (2) the feed rate was increased more slowly during the middle of the batch; (3) the feed rate was dropped back to zero much closer to the end of the batch; and (4) the final batch time was significantly longer. Both cases produced identical glucose feed concentration profiles in which the maximum value was selected for non-zero feed rates.

Figure 7 shows the liquid volume, glucose concentration and ethanol productivity trajectories when metabolite production occurred only in the G1 phase. The glucose concentration was driven to a much lower value than with ϕ_{G1} = 0 (see Figure 4). For this case maximization of fermentation relative to the other two metabolic pathways no longer represented the optimal solution. Instead the optimizer was forced to find a compromise between competing pathways: (1) fermentation that maximized the total cell number and the ethanol produced per cell in the G1 phase; and (2) glucose oxidation that maximized the number of cells in the G1 phase due to the effect of overall growth rate on the G1 phase duration. This interpretation is supported by Figure 8 which shows the cell number in each cell cycle phase and the growth rate attributable to each metabolic pathway for this case. As compared to the ϕ_{G1} = 0 case (see Figure 5), the optimal solution produced a lower overall growth rate such that the glucose oxidative and fermentative pathways had comparable growth rates. This shift in metabolic state produced a larger fraction of cells in the G1 phase, thereby compensating for the effects of decreased fermentative flux.

V. SUMMARY AND CONCLUSIONS

The problem of ethanol productivity optimization in fed-batch yeast fermenters was addressed by embedding a simple cell population model within a dynamic optimization strategy. The population model accounts for three metabolic pathways involved in ethanol production/consumption and the cell cycle dependency of ethanol production via the glucose fermentative pathway. Optimal fed-batch operating policies were determined by solving a dynamic optimization problem in which ethanol production was maximized subject to various constraints including the temporally discretized model equations. The proposed framework allows the comparison of optimal solutions obtained with different metabolite production rates in the G1, S and G2/M cell cycle phases.

We found that the optimal solution was most sensitive to the ethanol production rate in the G1 phase relative to the total production rate in the other cell cycle phases. Our results suggest that the impact of cell cycle dependent

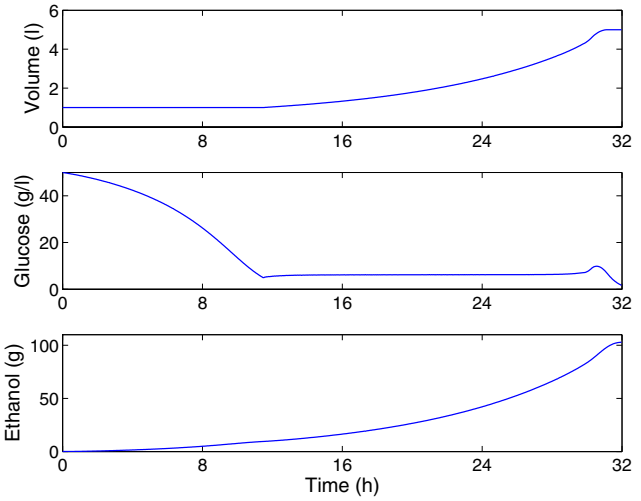

Fig. 7. Volume, glucose concentration and ethanol productivity obtained with the optimal feeding policy for metabolite production in the G1 cell cycle phase.

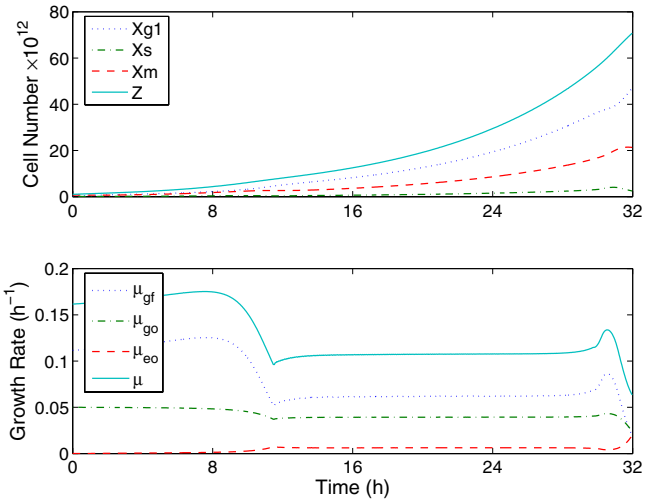

Fig. 8. Cell populations and growth rates obtained with the optimal feeding policy for metabolite production in the G1 cell cycle phase.

production is minimal for fermentation metabolites such as ethanol produced in the later phases. The proposed strategy appears to have greater potential for metabolic products and recombinant yeast proteins that are primarily synthesized and/or secreted during the G1 phase [21]. For this case the optimal solution will deviate substantially from that obtained with a standard model that neglects cell cycle production dependencies. Our future work will focus on further exploration of these hypotheses using more detailed population balance equation models that capture cell cycle dependent production of metabolites [10] and recombinant proteins.

VI. ACKNOWLEDGMENTS

The authors would like to acknowledge Victor Zavala and Larry Biegler (Carnegie Mellon University) for technical assistance with IPOPT and AMPL.

REFERENCES

[1] S. Ostergaard, L. Olsson, and J. Nielsen, "Metabolic engineering of *Saccharomyces cerevisiae*," *Microbiology and Molecular Biology Reviews*, vol. 64, pp. 34–50, 2000.

[2] B. R. Glick and J. J. Pasternak, *Molecular Biotechnology: Principles and Applications of Recombinant DNA*. Washington, DC: American Society for Microbiology, 1998.

[3] S. Frykman and F. Srienc, "Cell cycle-dependent protein secretion by *Saccharomyces cerevisiae*," *Biotechnol. Bioeng.*, vol. 76, pp. 259–268, 2001.

[4] K. Uchiyama, M. Morimoto, Y. Yokoyama, and S. Shioya, "Cell cycle dependency of rice α-amylase production in a recombinant yeast," *Biotechnol. Bioeng.*, vol. 54, pp. 262–271, 1997.

[5] R. A. Richieri, L. S. Williams, and P. C. Chau, "Cell cycle dependency of monoclonal antibody production in asynchronous serum-free hybridoma cultures," *Cytotechnology*, vol. 5, pp. 243–254, 1991.

[6] M. B. Gu, P. Todd, and D. S. Kompala, "Foreign gene expression (β-galactosidase) during the cell cycle phases in recombinant CHO cells," *Biotechnol. Bioeng.*, vol. 42, pp. 1113–1123, 1993.

[7] K. Uchiyama and S. Shioya, "Modeling and optimization of α-amylase production in a recombinant yeast fed-batch culture taking account of the cell cycle population distribution," *J. Biotechnol.*, vol. 71, pp. 133–141, 1999.

[8] D. E. Porro, B. Martegani, M. Ranzi, and L. Alberghina, "Oscillations in continuous cultures of budding yeasts: A segregated parameter analysis," *Biotechnol. Bioeng.*, vol. 32, pp. 411–417, 1988.

[9] C. Strassle, B. Sonnleitner, and A. Fiechter, "A predictive model for the spontaneous synchronization of *Saccharomyces cerevisiae* grown in continuous culture. I. Concept," *J. Biotechnol.*, vol. 7, pp. 299–318, 1988.

[10] P. Mhaskar, M. A. Henson, and M. A. Hjortso, "Cell population modeling and parameter estimation for continuous cultures of *Saccharomyces cerevisiae*," *Biotechno. Prog.*, vol. 18, pp. 1010–1026, 2002.

[11] W. Woehrer and M. Roehr, "Regulatory aspects of baker's yeast metabolism in aerobic fed-batch cultures," *Biotechnol. Bioeng*, vol. 23, 1981.

[12] A. Lubbert and S. B. Jorgensen, "Bioreactor performance: A more scientific approach for practice," *J. Biotechnology*, vol. 85, pp. 187–212, 2001.

[13] I. Y. Smets, J. E. Claes, E. J. November, G. P. Bastin, and J. F. V. Impe, "Optimal adaptive control of (bio)chemical reactors: Past, present and future," *J. Process Control*, vol. 14, pp. 795–805, 2004.

[14] A. Johnson, "The control of fed-batch fermentation – A survey," *Automatica*, vol. 23, pp. 691–705, 1987.

[15] K. Y. Rani and V. S. R. Rao, "Control of fermenters: A review," *Bioprocess Eng.*, vol. 21, pp. 77–88, 1999.

[16] L. T. Biegler, A. M. Cervantes, and A. Wachter, "Advances in simultaneous strategies for dynamic process optimization," *Chem. Eng. Sci.*, vol. 57, pp. 575–593, 2002.

[17] B. Sonnleitner and O. Kappeli, "Growth of *Saccharomyces cerevisiae* is controlled by its limited respiratory capacity: Formulation and verification of a hypothesis," *Biotechnol. Bioeng.*, vol. 28, pp. 927–937, 1986.

[18] M. A. Henson and D. E. Seborg, "Nonlinear control strategies for continuous fermentors," *Chem. Eng. Sci.*, vol. 47, pp. 821–835, 1992.

[19] J. E. Cuthrell and L. T. Biegler, "Simultaneous optimization and solution methods for batch reactor control problems," *Comput. Chem. Eng.*, vol. 13, pp. 49–62, 1987.

[20] A. Wachter and L. T. Biegler, "On the implementation of a primal-dual interior point filter line search algorithm for large-scale nonlinear programming," *Math. Progr.*, accepted.

[21] D. Perlman, P. Raney, and H. O. Halvorson, "Cytoplasmic and secreted *Saccharomyces cerevisiae* mRNAs encoded by one gene can be differentially or coordinatively regulated," *Mol. Cell. Biol.*, vol. 3, pp. 1682–1688, 1984.